16th World Conference on Earthquake Engineering, 16WCEE 2017

Santiago Chile, January 9th to 13th 2017

Paper N° 2891

Registration Code: S- I1464755271

COLLAPSE SIMULATION OF NON DUCTILE RC FRAME BUILDING

Anil Suwal [(1)], Adolfo Matamoros [(2)], Andres Lepage [(3)]

[(1)] *Graduate Research Assistant, University of Texas at San Antonio, anil.suwal@utsa.edu*
[(2)] *Peter T. Flawn Professor, University of Texas at San Antonio, abm@utsa.edu*
[(3)] *Associate Professor, University of Kansas, alepage@ku.edu*

Abstract

This paper presents collapse simulation results from three analytical models of a non-ductile reinforced concrete moment frame building that was severely damaged during the 1994 Northridge earthquake. The three models were developed using the open source software platform OpenSees, using the same configuration and different modeling parameters for moment frame columns and beams. Modeling parameters for columns were calculated using the provisions in ASCE 41-13 or new column provisions proposed by ACI Committee 369. Modeling parameters for moment frame beams were calculated using the provisions in ASCE 41-13 or new provisions derived by the authors based on experimental results. Modeling parameters for slab-column connections were calculated using the provisions in ASCE 41-13 for all building models. Models were calibrated using motions recorded at the building site, and used to perform incremental dynamic analyses to evaluate the effect of modeling parameters on the calculated collapse intensity and collapse mechanism of the building. All models developed lateral instabilities due to two-story mechanisms involving the fourth and fifth floors signaled by a very abrupt change in the slope of the relationship between the Intensity Measure and the Maximum Story Drift ratio. This type of behavior was associated with a large number of columns in the fifth floor experiencing shear failure and developing negative slopes in their force-deformation curves. The intensity measure at collapse was affected significantly by changes in the modeling parameters defining the capping rotation and the drift ratio corresponding to total loss of lateral stiffness of the columns, and was not sensitive to changes in the modeling parameters of the beams.

Keywords: collapse, earthquake, modeling parameter, nonlinear dynamic analysis, reinforced concrete,

1. Introduction

Modeling parameters in the FEMA 356 [1] pre-standard and ASCE 41-06 [2] standard were developed by relying primarily on engineering judgement because at the time these documents were published there was very little experimental data on the behavior of reinforced-concrete members beyond the loss of lateral load capacity. A greater level of conservatism was adopted for modes of failure that were brittle in nature or had potentially catastrophic consequences due to the high level of uncertainty inherent in the modeling parameters. During the last 10 years, the number of experimental studies has increased, and significant efforts have been made to incorporate this information into evaluation standards by developing modeling parameters that reflect the physical behavior of reinforced-concrete members more accurately.

The first significant change in the modeling parameters of the ASCE 41 standard was implemented in 2007 through an addendum developed to incorporate results from studies on the potential for collapse of RC structures [3]. Although the modeling parameters for reinforced concrete columns introduced in the addendum were based on statistical analyses of test results, the prevailing philosophy of the standard remained to adopt modeling parameters with a significant level of conservatism – 35% probability of exceedance for columns in which shear failure occurred after flexural yielding and 15% probability of exceedance for shear-critical columns in the calibration data set – instead of providing modeling parameters representative of median values.

That modeling philosophy changed with the development of new column modeling parameters by ACI Committee 369 [4]. These proposed modeling parameters for columns are based on a 50% probability of exceedance regardless of the mode of failure. The reasoning behind the change in modeling approach is that modeling parameters should be used to estimate the expected behavior of buildings as accurately as possible, while the level of conservatism should be assigned through acceptance criteria. Changes in modeling parameters for reinforced concrete columns implemented during the last ten years are very significant, although there is very little information on the effect of those changes on the calculated response of building systems. The goal of this paper is to address that knowledge gap by evaluating the effect of using different sets of modeling parameters on the response of an existing nonductile reinforced concrete building structure. The case-study structure was selected because it was instrumented and acceleration records were available from several strong earthquakes, including the 1994 Northridge earthquake. Although the nonlinear dynamic assessment methodology in ASCE 41 relies on acceptance criteria and does not address the potential for collapse of the structure, this paper focuses on simulating the nonlinear response of the structure up to the point of collapse as a means to investigate the validity of different sets of modeling parameters for the entire range of nonlinear response. These types of simulations are important because they can provide a more accurate assessment of the risk of collapse of buildings and because there are many challenges associated with modeling the nonlinear behavior of reinforced concrete structures in which columns experience shear failure. Building models of this kind can be used to understand the most important characteristics that can cause the collapse of nonductile reinforced concrete buildings under a combination of gravity and seismic loads.

2. Building Description

The case study building is a seven-story reinforced concrete structure located in Van Nuys, California which was designed in 1965. The building has a total height of 65.6 ft. It is rectangular in plan with eight-bay frames in the east-west direction and three-bay frames in the north-south direction. The building was constructed with normal weight concrete and the gravity system consists of interior reinforced concrete flat slabs and perimeter spandrel beams supported by concrete columns. Lateral forces are resisted mainly by spandrel beam-column perimeter frames. The concrete slab is 10-in. thick at the second floor, 8.5-in. thick at the third to seventh floors, and 8-in. thick at the roof. Typical column dimensions are 14 x 20 in. with the weak bending axis oriented in the east-west direction. The foundation system consists of cast-in-place concrete friction piles with caps connected by foundation beams below grade. The ground floor had masonry infill walls separated from the perimeter frames by one-in. expansion joints. A detailed description of element dimensions and reinforcement is presented by Suwal [5].

The building was instrumented with a total of sixteen sensors and strong motion records available from California Strong Motion Instrumentation Program (CSMIP) through the CESMD database [6]. The building sustained extensive damage in beams, columns, and beam-column joints during the 1994 Northridge earthquake. The most severe structural damage was observed at the top of the fourth story of the east-west perimeter frame. The north-south perimeter frames sustained limited damage mostly in the form of flexural cracks.

3. Analytical Model

This paper presents results from two-dimensional analyses of the building response in the east-west direction, where the most severe damage occurred during the Northridge earthquake. The two-dimensional models evaluated include one perimeter frame and one interior frame, representing half the lateral-load and gravity-load resisting systems of the building in the east-west direction. Both frames were modeled using a lumped-plasticity approach with elastic beam-column elements and zero-length rotational springs to represent the nonlinear behavior of the structure. Nonlinear spring elements representing plastic hinges were offset from the centerlines of the frames and connected with flexible linear-elastic elements to simulate the flexibility of the joints. A leaning column was used to account for the destabilizing P-delta effects of gravity loads not directly applied to the frames. All building models had the same configuration, with the only difference between them being the modeling parameters of the zero-length spring elements of beams and columns in the perimeter frame. Building models were developed with the goal of reasonably simulating the behavior of the structural elements up to the stage of building collapse. OpenSees (Open System of Earthquake Engineering Simulation) [7], a framework for earthquake engineering simulation developed by PEER (Pacific Earthquake Engineering Research), was employed to conduct the analyses.

The layout of the frames is shown in Fig. 1, which illustrates the location of nodes, elastic beam-column elements, zero length springs, and joint offset elements. Each of the zero-length spring elements was connected to two different nodes at the same location, as shown in Fig. 1 (to the right of the frame).

The nonlinear behavior of the rotational springs was defined using a uniaxial material model originally developed by Ibarra[8], implemented into the OpenSees platform by Altoontash [9], and modified by Lignos [10]. The material model used is designated in OpenSees as the Modified Ibarra-Medina-Krawinkler model. As shown in Fig. 2, the model has a trilinear backbone curve and can be used to model both monotonic and cyclic deterioration. The key parameters of the model are the elastic stiffness (K_e), the yield moment (M_y), the ratio of capping to yield moment (M_c/M_y), the plastic rotation capacity in post yield region (θ_p), the post capping rotation capacity (θ_{pc}), the ultimate rotation (θ_u), and the degradation parameters.

For nonlinear cyclic behavior, the material model captures four basic modes of deterioration: basic strength deterioration, post-capping deterioration, accelerated reloading stiffness deterioration, and unloading stiffness deterioration. Cyclic deterioration uses an energy index that has two parameters: normalized energy dissipation capacity and an exponent term to define the rate of deterioration with accumulation of damage. Values for the deterioration parameters were derived based on a calibration using 255 experimental tests by Haselton [11].

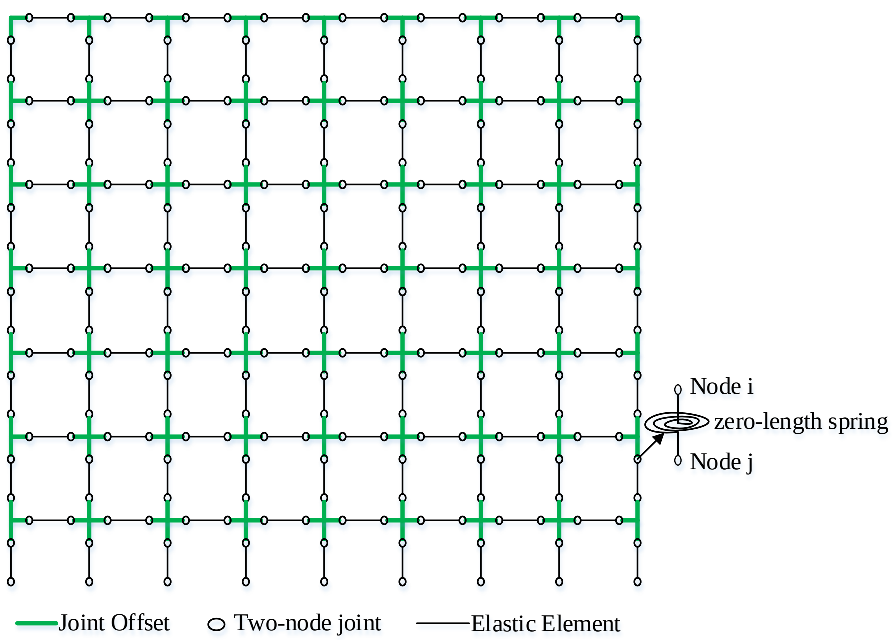

Figure 1: Analytical model of a typical frame in the east-west direction

Building response was analyzed using three different models designated A, B and C. Modeling parameters for all elements in model A were calculated following the provisions in the ASCE 41-13 [12] Standard. Modeling parameters for columns in Model B were calculated using the ACI 369 guidelines, while all other modeling parameters were calculated using the provisions in ASCE 41-13. Column modeling parameters in model C were calculated using the ACI 369 guidelines, while modeling parameters for spandrel beams were determined using new guidelines developed using experimental results from beam tests. The three sets of modeling parameters are described below.

3.1 Model A

The shape of the backbone curve prescribed in Chapter 10 of the ASCE 41-13 Standard is shown in Figure 3. Modeling parameters *a*, *b*, and *c* are used to define the inelastic rotation corresponding to loss of lateral load capacity, the inelastic rotation corresponding to total loss of lateral load capacity (which has been experimentally shown to coincide with axial failure for columns), and the residual strength after loss of lateral load capacity. The initial stiffness for spandrel beams and columns was defined using the effective stiffness criteria for beams and columns in ASCE 41-13, including the effects of the slab. Slab width used to calculate effective stiffness of the beams was set equal to the width of the column strip. Yield moment for the rotational springs was calculated using moment-curvature relationships computed using a longitudinal reinforcement yield strength equal to 1.25 times the nominal strength and concrete strength equal to 1.5 times the specified compressive strength.

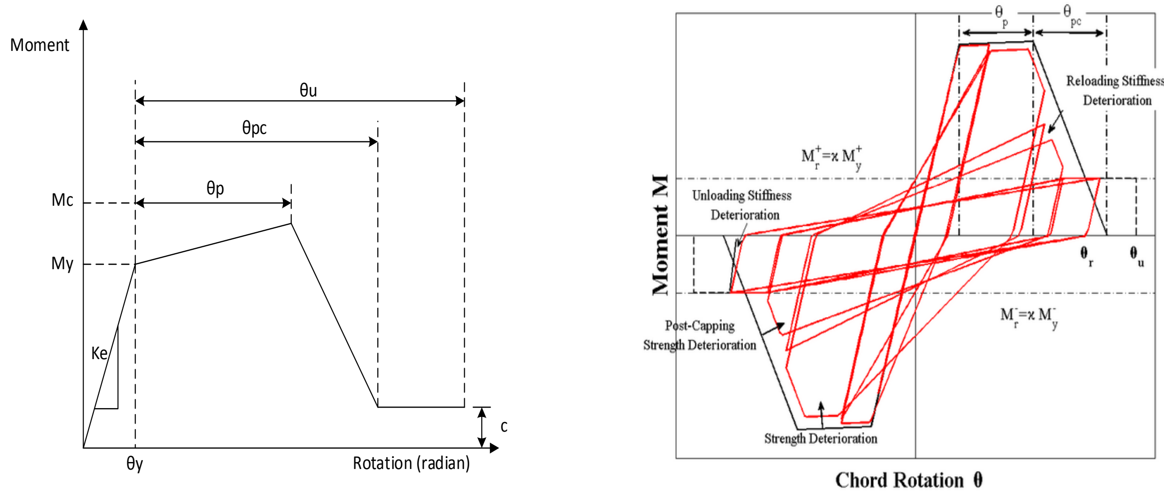

(a) (b)

Figure 2: Material model for rotational spring (a) monotonic (b) cyclic

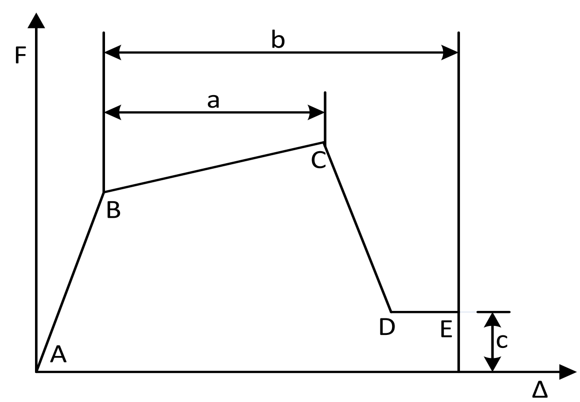

Figure 3: ASCE 41-13 backbone curve for deformation-controlled members

The capacity of beam and column members in shear were determined according to the provisions in ACI 318-14 [13] and ASCE 41-13. The modeling parameters for columns are dependent on the ratio of nominal shear strength to the plastic shear demand, and the type of anchorage detailing of the longitudinal and transverse reinforcement, as specified in ASCE 41-13.

The interior slab-column frame was modeled using beam-column elements. The effective beam width model was used with an effective beam width factor of 0.48 and an effective stiffness factor of 0.33, to take into account the effects of slab cracking. Following the provisions in ASCE 41-13, these values were calculated based on recommendations by Hwang and Moehle [14].

3.2 Model B

Modeling parameters for the interior and exterior columns of Model B were calculated using the new provisions proposed by ACI Committee 369 (Eq. 1, 2, and 3).

$$a_{nl} = 0.042 - 0.043\frac{N_{UD}}{A_g f'_{cE}} + 0.63\rho_t - 0.023\frac{V_{yE}}{V_{OE}} \geq 0.0 \tag{1}$$

$$b_{nl} = \frac{0.5}{5+\frac{N_{UD}}{0.8A_g f'_{cE}}\frac{1}{\rho_t}\frac{f'_{cE}}{f_{ytE}}} - 0.01 \geq a_{nl} \tag{2}$$

$$c_{nl} = 0.24 - 0.4\frac{N_{UD}}{A_g f'_{cE}} \geq 0.0 \quad (3)$$

where a_{nl}, b_{nl}, and c_{nl} are the inelastic rotation corresponding to capping in units of radians, the inelastic rotation corresponding to total loss of lateral load capacity in radians, and the residual strength ratio of the column element, respectively. The term f'_{cE} is the expected concrete compressive strength, in units of ksi, N_{UD} is the axial force in kips, A_g gross sectional area of the column in in^2, ρ_t is shear reinforcement ratio, and V_{yE} and V_{oE} are the expected values of plastic shear demand and the nominal shear demand in kips, respectively.

Calculations showed that inelastic rotations corresponding to the capping point determined using the recommendations by ACI Committee 369 were approximately 0.01 radians larger than values calculated with the provisions of ASCE 41-13. Calculated inelastic rotations corresponding to total loss of lateral load capacity were also larger for the ACI 369 provisions than the ASCE 41-13 Standard. A comparison between backbone curves determined using modeling parameters in ASCE 41-13 and the ACI 369 recommendations for a representative column and spandrel beam elements are shown in Figure 4. As the figure shows, for this particular building the change in modeling parameters for columns had a very significant effect on the inelastic rotations corresponding to total loss of lateral load capacity.

3.3 Model C

In this model, modeling parameters for columns were the same as Model B, i.e. modeling parameters for exterior and interior columns were determined using the recommendations of ACI Committee 369 while modeling parameters for slab-column connections were determined using the provisions in the ASCE 41-13 Standard. New recommendations for beams were determined based on experimental results and the provisions for columns. An expression for the total rotation corresponding to capping was developed based on linear regression from 56 specimens from the PEER database with axial load ratios ranging between 0 and 0.12. Because there are very few experimental results that track the response of beam specimens to the point of total loss of lateral load capacity, a recommendation was developed by evaluating an axial load ratio corresponding to an axial load ratio of 10% in the equation proposed by ACI Committee 369 for columns.

$$a_{nl} = 0.12\sqrt{\rho_t \frac{f_{ytE}}{f'_{cE}}} + \frac{L}{600\,h} - \frac{s}{1400\,d_b} + \frac{V}{300\,b\,d\sqrt{f'_{cE}}} - \theta_y \geq 0.0 \quad (4)$$

$$b_{nl} = \frac{0.5}{5 + \frac{0.1\,f'_{cE}}{f_{ytE}}\frac{1}{\rho_t}\frac{h}{d_c}} - \theta_y \geq a_{nl} \quad (5)$$

where a_{nl} and b_{nl} are the inelastic rotations corresponding to the capping point and total loss of load capacity, in radians, f_{ytE} is the expected yield strength of the transverse reinforcement in psi, f'_{cE} is the expected concrete compressive strength in psi, L is the clear span of the beam, h is the beam depth, s is the transverse reinforcement spacing, d_b is the longitudinal bar diameter, d_c is the depth of the beam core, V is the shear strength of the beam in lbs, ρ_t is the transverse reinforcement ratio, and b is the width of the beam in in.

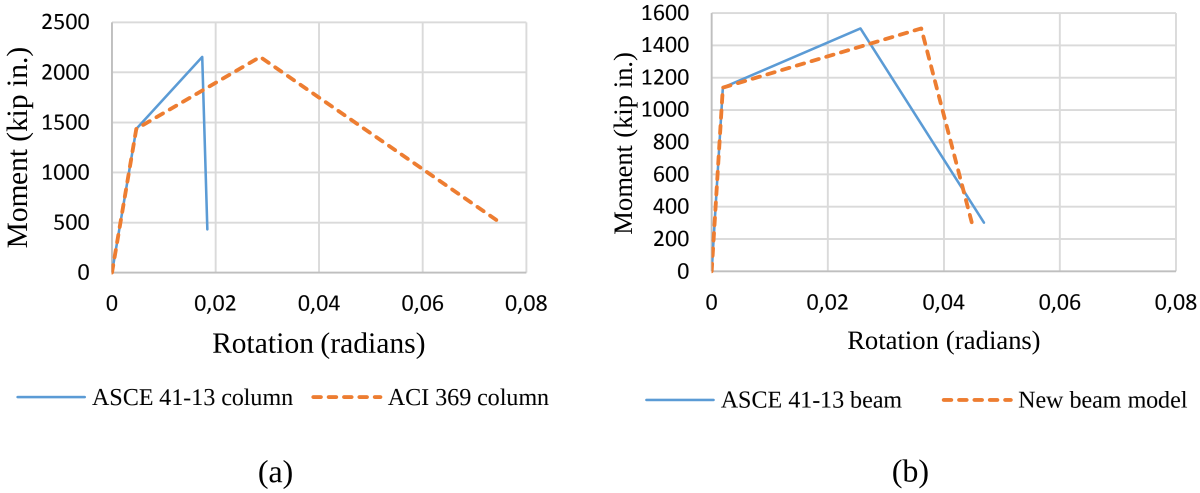

Figure 4: Comparison between ASCE 41-13 and ACI 369 backbone curves for a) representative column b) representative spandrel beam

While the results correlate very well with the experimental data set, the difference between the backbone curves calculated with the proposed equation and the ASCE 41-13 Standard was not very significant for the spandrel beam members in this building due to the low amount of transverse reinforcement. Modeling parameters for spandrel beams calculated using the proposed equations were approximately 0.01 radians larger for the inelastic rotation at capping, and almost same for the inelastic rotation corresponding to total loss of lateral load capacity.

4. Building Analyses

The three analytical models were used to perform nonlinear dynamic analyses using OpenSees. The fundamental period of vibration calculated with the models was similar to periods reported by other researchers for this building. Because the strongest earthquake recorded at the site was the 1994 Northridge earthquake, the ground motion recorded at the base of the building for this earthquake was used to perform all nonlinear dynamic analyses presented in this paper. The peak horizontal acceleration of the Northridge earthquake recorded at the base of the building was 0.47g. The analysis was performed for 60 seconds of the ground motion record using 2% Rayleigh viscous damping. Figure 5 shows the calculated and recorded relative roof displacement response. The recorded relative roof displacement response was derived from the strong motion data recorded at the building by CSMIP and available in the CESMD database [6]. As shown in Fig. 5, the calculated response for the three models at this intensity was approximately the same, and in all cases correlated well with the building response.

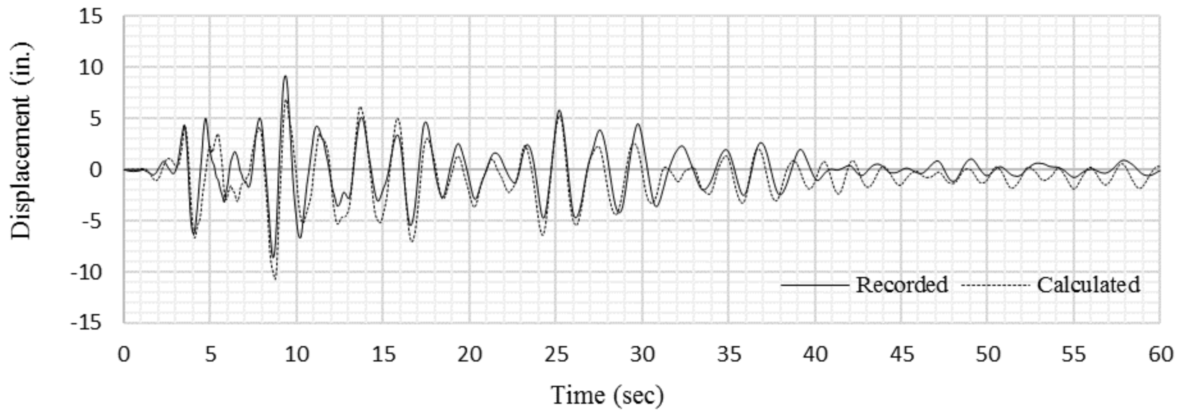

Figure 5: Recorded and calculated relative roof displacement

5. Results from Incremental Dynamic Analysis

Incremental dynamic analysis (IDA)[15] is a technique in which a structural model is subjected to increasing levels of ground motion intensity, until the building develops lateral instability. As stated previously, all the analyses presented in this paper were performed using the strong motion recorded at the base of the building during the 1994 Northridge earthquake. The ground motion was scaled with factors starting at 0.05, in increments of 0.05, until the behavior of the model became unstable due to excessive lateral deformations. Calculated drift ratios for approximately 300 nonlinear dynamic analyses of the three models are summarized in Figs. 6 through 12.

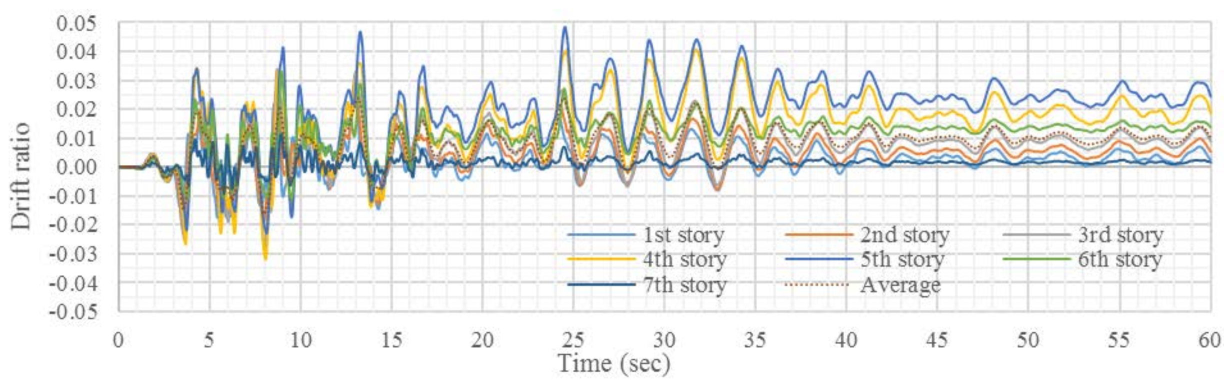

Figure 6: Calculated story drift ratios for model B at IM 2.72, near lateral instability

Figures 5, 6 and 7 show the typical progression in building behavior that was observed in the analyses. As the intensity measured increased, displacement demands corresponding to the peaks between 8 and 10 seconds (Fig. 5, IM 1.0) induced very severe damage in the building columns. This effect is shown in Fig. 6 for an intensity measure near lateral instability, where the heavy damage to the columns is reflected by the permanent deformations at the end of the analysis and the fact that peak story drift ratios calculated between 24 and 35 seconds were as high as those recorded during the first 10 seconds. Eventually the damage inflicted during the first 10 seconds of the record was so severe that the 4th and 5th stories developed story mechanisms and became unstable, at an IM of 2.73 for model B (Fig. 7).

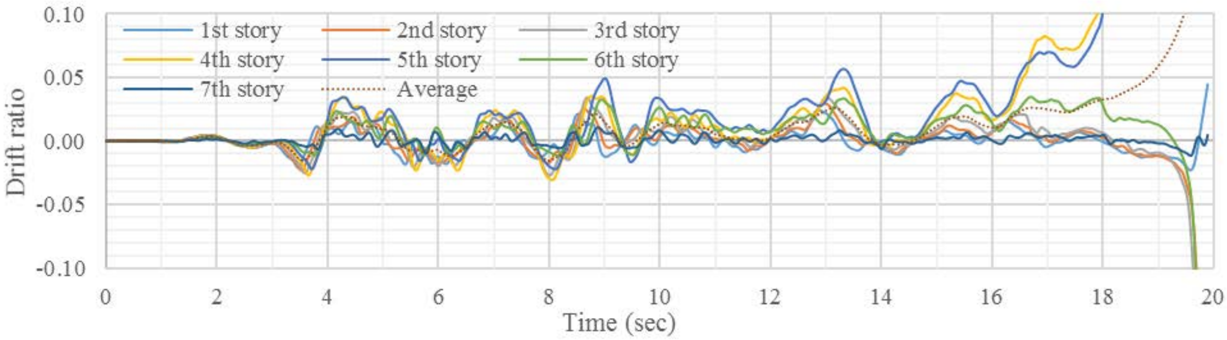

Figure 7: Calculated story drift ratios for model B analysis at IM 2.73, which corresponded to lateral instability

5.1 Model A

Figure 8a shows the results of the IDA for the case study building with the ASCE 41-13 modeling parameters. At an intensity measure of 1.63 times the Northridge ground motion (PGA of 0.77 g), the story drift ratio of the 5th increased significantly, indicating the formation of a story mechanism, and the curve flattened out, indicating that the building would collapse due to lateral instability. The curve for the 4th story reaches a plateau similarly to the 5th story. The maximum story drift ratio for the building model at the verge of collapse was approximately 3.2%, and the average drift ratio was approximately 2%.

5.2 Model B

The IDA curve for model B is shown in Fig. 8b. In this case the story drift curve for the 5th story became nearly flat, indicating lateral instability, at intensity measure of 2.73 (PGA of 1.28 g). The maximum story drift ratio prior to collapse was approximately 4.5%. Both of these values are significantly higher (60% increment in intensity measure and 40% increment on the drift ratio) than those corresponding to collapse for the model with the ASCE 41-13 modeling parameters, although the increment in average drift ratio for the building was modest (2.2% vs. 2%). The curves for story drift indicate that a story mechanism formed in the 5th story closely followed by a story mechanism in the 4th story.

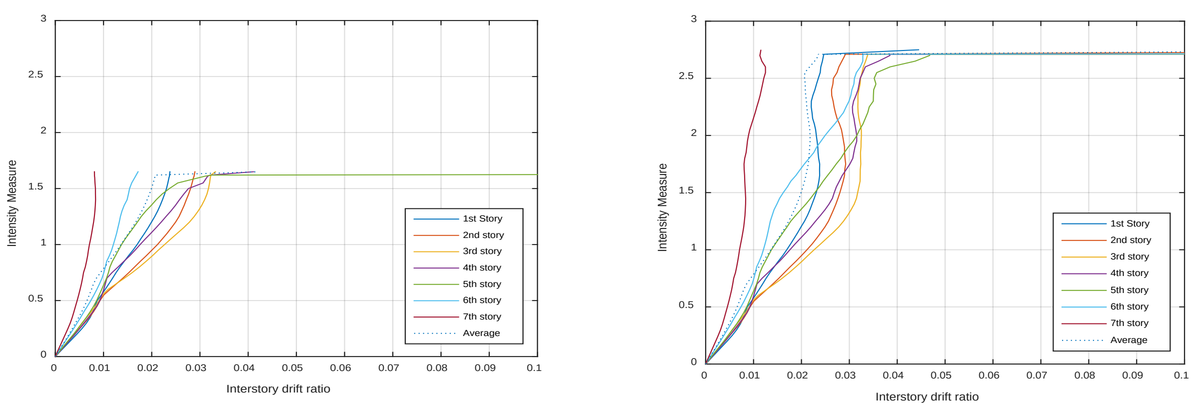

a) Model A   b) Model B

Figure 8: IDA curves for models A and B

5.3 Model C

Figure 9 shows the IDA curve for model C. The behavior was very similar to that of model B, although the maximum story drift ratio in the fifth story reached approximately 5.5% before the building developed lateral instability. The intensity measure corresponding to lateral instability for model C was slightly lower than model B (2.72 vs. 2.73) and the average drift ratio near collapse was approximately 2.5%. Although the use of median modeling parameters for the spandrel beams of the perimeter frame led to larger story deformations prior to collapse, those larger story deformations placed a greater deformation demand on the columns and slightly reduced the IM corresponding to lateral instability. Figure 9 shows that the first story to develop a mechanism was the 5th, followed by the 6th and the 4th.

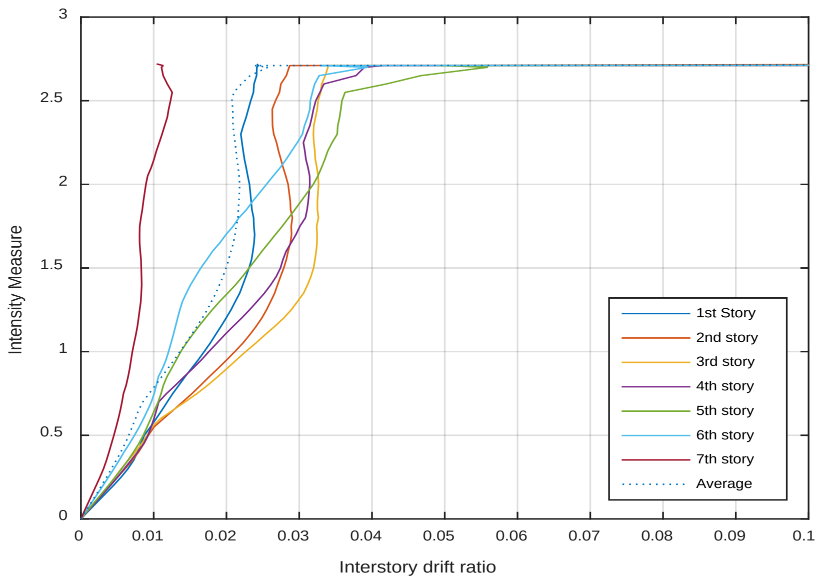

Figure 9: IDA curve for Model C

The distribution of damage in the three models near collapse is shown in Fig. 10 to 12. In these figures, hinge location in which the rotation demand was between the yield and capping points (stable behavior) are shown in green, and hinge locations in which the rotation demand exceeded the capping point (unstable behavior and high likelihood of axial failure in columns and slab-column connections of the interior frame) are shown in white. These figures illustrate one of the limitations of the analyses and one of the most challenging aspects of estimating the intensity measure corresponding to collapse. Deformation demands exceeding capping can cause localized collapse that could precipitate the global collapse of the structure. The computer models used in the analysis do not recognize the effect of these localized failures on the ability of the structure to carry gravity loads, and only reflect the loss of lateral load capacity.

Figure 10a shows that for model A, at an intensity measure near lateral instability, most of the columns in the fifth floor of the perimeter frame would have experienced shear failure and likely axial failure also. Damage to the interior frame lab-column connections is also expected to be very severe, with high likelihood of punching shear failures. The larger nonlinear modeling parameters *a* and *b* used in the columns of models B and C caused yielding to spread over a larger number of columns prior to developing lateral instability, although the pattern of damage to the columns of the fifth floor remained very similar. Another outcome of increasing the modeling parameters of the columns in the perimeter frame is that the damage to the slab-column connections of the interior frame (Fig. 11b) became much more severe and spread out over a larger number of connections. A comparison between Figs. 10 and 11 shows that the increase in modeling parameters *a* and *b* for the spandrel beams of the exterior frame caused a few beams to remain in the stable range prior to collapse, placing a greater deformation demand on the columns and slightly increasing the base shear capacity of the structure.

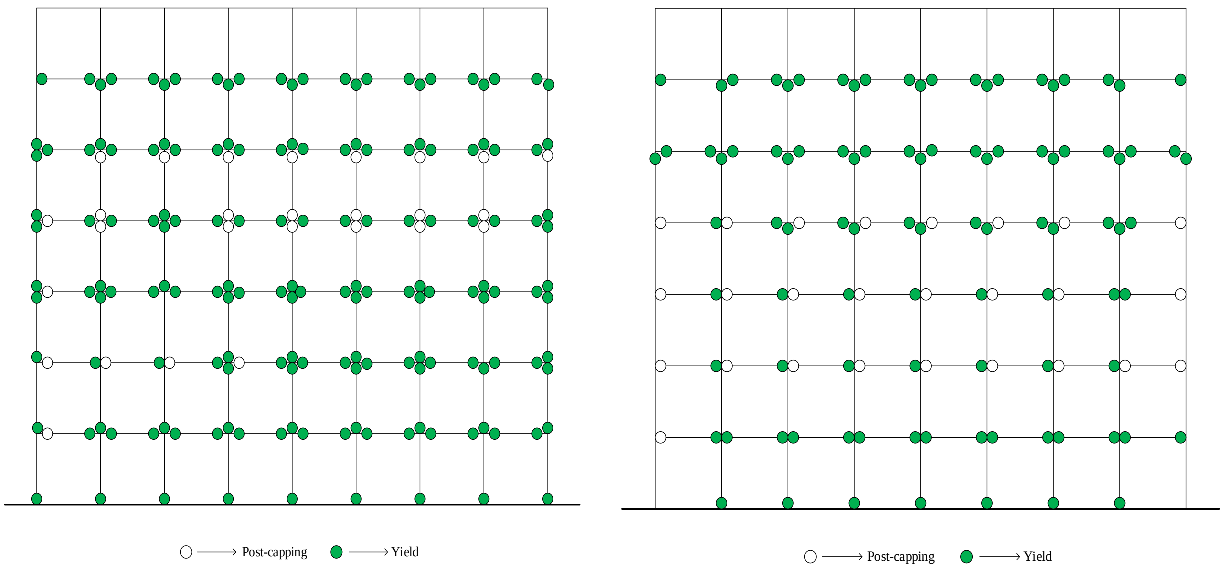

(a) (b)

Figure 10: Damage distribution for model A, a) Exterior frame b) Interior frame

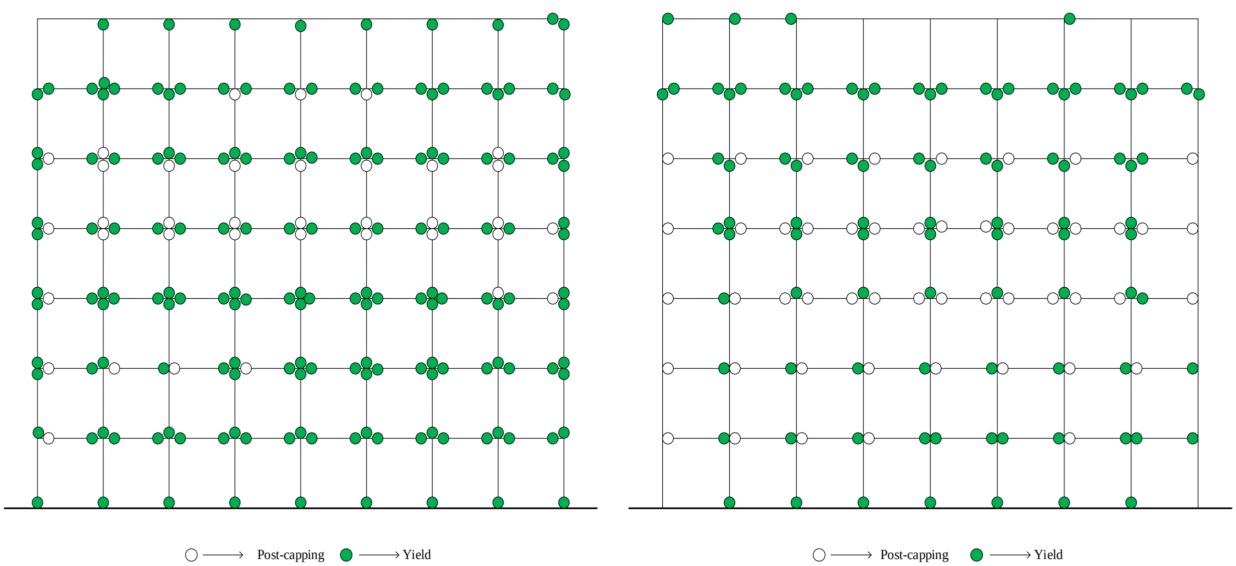

(a) (b)

Figure 11: Damage distribution for model B, a) Exterior frame b) Interior frame

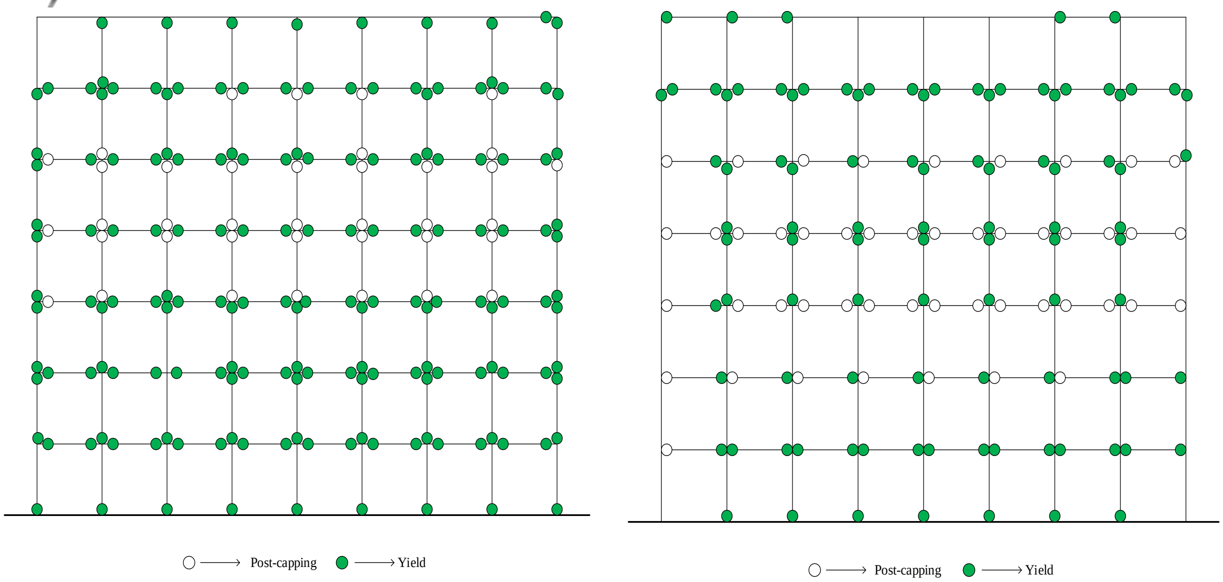

(a) (b)

Figure 12: Damage distribution for model C, a) Exterior frame b) Interior frame

6. Conclusions

On the basis of the analytical results presented, the following conclusions are drawn:

- The intensity of ground shaking that the building was able to sustain significantly increased when the new modeling parameters for columns proposed by ACI Committee 369 were used instead of those specified in ASCE 41-13. The intensity measure corresponding to lateral instability for the model with ASCE 41-13 modeling parameters was 1.63 (0.77 g), whereas the maximum intensity measure for the model with ACI 369 modeling parameters was 2.71 (1.27 g).
- The story drift ratio corresponding to lateral instability for the two models with ACI 369 modeling parameters for columns were significantly higher than the story drift ratio for the model with ASCE 41-13 modeling parameters for columns (4.6% vs. 3.2%)
- The effect of using median values for beam modeling parameters on the behavior of the building near collapse was very minor (the intensity measure corresponding to lateral instability was nearly the same for models B and C).
- The maximum story drift ratio at lateral instability for model C, with beam modeling parameters corresponding to median values from experimental data, was the highest of the three models (5.5% for model C vs. 4.6% for model B).

Acknowledgements

The authors would like to acknowledge the support of the National Science Foundation under award number 0618804 through the Pacific Earthquake Engineering Research Center (PEER).

References

[1] Federal Emergency Management Agency. 2000. “Prestandard and Commentary for the Seismic Rehabilitation of Buildings, FEMA 356.” Washington, D.C., November 2000.

[2] ASCE/SEI, 2006, "Seismic Rehabilitation of Existing Buildings (ASCE/SEI 41-06)," American Society of Civil Engineers, Reston, VA

[3] Elwood, K., Matamoros, A., Wallace, J., Lehman, D., Heinz, J., Mitchell, A., Moore, M., Valley, M., Lowes, L., Comartin, C., Moehle, J., 2007. “Update to ASCE/SEI 41 Concrete Provisions”, Earthquake Spectra, Journal of the Earthquake Engineering Research Institute, Vol. 23, No. 3, pp. 493-523.

[4] Ghannoum, W., and Matamoros, A., 2014. “Nonlinear Modeling Parameters and Acceptance Criteria for Concrete Columns”, American Concrete Institute Special Publication, 297, 1-24.

[5] Suwal, A., 2015. "Evaluation of Modeling Parameters in ASCE 41-13 for the Nonlinear Static and Dynamic Analysis of an RC Building," M.S. Thesis, Department of Civil and Environmental Engineering, University of Texas at San Antonio, San Antonio, TX.

[6] CESMD, Center for Engineering Strong Motion Data, www.strongmotioncenter.org

[7] Mazzoni, S., McKenna, F., Scott, M. H., and Fenves, G. L., 2006, "OpenSees command language manual," *Pacific Earthquake Engineering Research (PEER) Center*, University of California, Berkeley.

[8] Ibarra, L. F., Medina, R. A., and Krawinkler, H., 2005 "Hysteretic models that incorporate strength and stiffness deterioration," *Earthquake Engineering & Structural Dynamics*, vol. 34, pp. 1489-1511, 2005.

[9] Altoontash, A., 2004, "Simulation and Damage Models for Performance Assessment of Reinforced Concrete Beam-Column Joints," PhD Thesis, Department of Civil and Environmental Engineering, Stanford University, Stanford, California.

[10] Lignos, D. and Krawinkler, H., 2008, "Sidesway Collapse of Deteriorating Structural Systems under Seismic Excitations," PhD Thesis, Department of Civil and Environmental Engineering, Stanford University, Stanford, California.

[11] Haselton, C. B., Liel, A., Taylor, S., and Deierlein, G., 2008 "Beam-Column Element Model Calibrated for Predicting Flexural Response Leading to Global Collapse of RC Frame Buildings," PEER Report 2007/03: Pacific Earthquake Engineering Research Center, College of Engineering, University of California, Berkeley.

[12] ASCE/SEI, 2014, "Seismic Evaluation and Retrofit of Existing Buildings (ASCE/SEI 41-13)," American Society of Civil Engineers, Reston, VA.

[13] ACI Committee 318, "Building Code Requirements for Structural Concrete (ACI 318-14) and Commentary," American Concrete Institute, Farmington Hills, MI, 2014, 520 pp.

[14] Hwang, S.-J., and Moehle, J. P., 2000, "Models for laterally loaded slab-column frames," *ACI Structural Journal*, V. 97, pp. 345-352.

[15] Vamvatsikos, D. and Cornell, C. A., 2002, "Incremental Dynamic Analysis," *Earthquake Engineering & Structural Dynamics*, V. 31, pp. 491-514.